

High potential for CH₄ emission mitigation from oil infrastructure in one of EU's major production regions

Foteini Stavropoulou^{1,*}, Katarina Vinković^{2,*}, Bert Kers², Marcel de Vries², Steven van Heuven², Piotr Korbeń³, Martina Schmidt³, Julia Wietzel³, Pawel Jagoda⁴, Jaroslav M. Necki⁴, Jakub Bartyzel⁴, Hossein Maazallahi¹, Malika Menoud¹, Carina van der Veen¹, Sylvia Walter¹, Béla Tuzson⁵, Jonas Ravelid⁵, Randolph Paulo Morales⁵, Lukas Emmenegger⁵, Dominik Brunner⁵, Michael Steiner⁵, Arjan Hensen⁶, Ilona Velzeboer⁶, Pim van den Bulk⁶, Hugo Denier van der Gon⁶, Antonio Delre⁷, Maklawe Essonanawe Edjabou⁷, Charlotte Scheutz⁷, Marius Corbu^{8,9}, Sebastian Iancu⁹, Denisa Moaca⁹, Alin Scarlat^{8,9}, Alexandru Tudor^{8,9}, Ioana Vizireanu⁹, Andreea Calcan⁹, Magdalena Ardelean⁹, Sorin Ghemulet⁹, Alexandru Pana⁹, Aurel Constantinescu⁹, Lucian Cusa⁹, Alexandru Nica⁹, Calin Baciu¹⁰, Cristian Pop¹⁰, Andrei Radovici¹⁰, Alexandru Mereuta¹⁰, Horatiu Stefanie¹⁰, Alexandru Dandocsi¹¹, Bas Hermans¹², Stefan Schwietzke¹³, Daniel Zavala-Araiza^{1, 13}, Huilin Chen^{2, 14**}, Thomas Röckmann^{1,**}

¹Institute for Marine and Atmospheric Research Utrecht (IMAU), Utrecht University, the Netherlands

²Centre for Isotope Research (CIO), Energy and Sustainability Research Institute Groningen, University of Groningen, The Netherlands

³Institute of Environmental Physics, University of Heidelberg, Heidelberg, Germany

⁴Faculty of Physics and Applied Computer Science, AGH University of Science and Technology in Cracow, Cracow, Poland

⁵Laboratory for Air Pollution/Environmental Technology, Empa – Swiss Federal Laboratories for Materials Science and Technology, Überlandstrasse 129, CH-8600 Dübendorf

⁶Department of Environmental Modelling, Sensing & Analysis, TNO, the Netherlands

⁷Department of Environmental Engineering, Technical University of Denmark, Denmark

⁸ Faculty of Physics, University of Bucharest, P.O. Box MG-11, Măgurele, 077125, Bucharest, Romania

⁹ National Institute for Aerospace Research “Elie Carafoli” – INCAS Bucharest, Romania

¹⁰Faculty of Environmental Science and Engineering, Babes-Bolyai University, Cluj-Napoca, Romania

¹¹National Institute of Research and Development for Optoelectronics, Măgurele, Romania

¹² Intero - The Sniffers, Poeierstraat 14, 2490 Balen, Belgium

¹³Environmental Defense Fund, Berlin, Germany and Amsterdam, The Netherlands

¹⁴Joint International Research Laboratory of Atmospheric and Earth System Sciences, School of Atmospheric Sciences, Nanjing University, Nanjing, China

* These authors contributed equally to the manuscript

** corresponding authors

Abstract

Ambitious methane (CH₄) emissions mitigation represents one of the most effective opportunities to slow the rate of global warming over the next decades. The oil and gas (O&G) sector is a significant source of methane emissions, with technically feasible and cost-effective emission mitigation options. Romania, a key O&G producer within the EU, with the second highest reported annual CH₄ emissions from the energy sector in year 2020 (Greenhouse Gas

48 Inventory Data - Comparison by Category, 2022), can play an important role towards the EU's
49 emission reduction targets. In this study, we quantify CH₄ emissions from onshore oil
50 production sites in Romania at source and facility level using a combination of ground and
51 drone-based measurement techniques. Measured emissions were characterised by heavily
52 skewed distributions, with 10% of the sites accounting for more than 70% of total emissions.
53 Integrating the results from all site-level quantifications with different approaches, we derive
54 a central estimate of 5.4 kg h⁻¹ site⁻¹ of CH₄ (3.6 – 8.4, 95% confidence interval) for oil
55 production sites. This estimate represents the third highest when compared to measurement-
56 based estimates of similar facilities from other production regions. Based on our results, we
57 estimate a total of 120 ktons CH₄ yr⁻¹ (range: 79 - 180 ktons yr⁻¹) from oil production sites in
58 our studied areas in Romania. This is approximately 2.5 times higher than the reported
59 emissions from the entire Romanian oil production sector for 2020. Based on the source level
60 characterization, up to three quarters of the detected emissions from oil production sites are
61 related to operational venting. Our results suggest that O&G production infrastructure in
62 Romania holds a massive mitigation potential, specifically by implementing measures to
63 capture the gas and minimize operational venting and leaks.

64 **Keywords:** Methane emissions; Oil and gas sector; Emissions distributions; Ground-based
65 measurements; Romania; Mitigation;

66 1. Introduction

67 CH₄, a potent greenhouse gas, is more effective at trapping radiation than CO₂, but has a
68 shorter lifetime. CH₄ is responsible for at least 25% of current global warming (Ocko et al.,
69 2021; Szopa et al., 2021). A 45% reduction in anthropogenic CH₄ emissions by 2030 would
70 avoid 0.25 °C in global warming by mid-century (Ocko et al., 2021), increasing the feasibility of
71 achieving the Paris Agreement goal.

72 CH₄ is emitted from a variety of anthropogenic and natural sources. Anthropogenic sources
73 account for 50–65% of total CH₄ emissions (Saunio et al., 2020), with approximately one third
74 of global anthropogenic CH₄ emissions originating from the fossil fuel-sector (i.e., emissions
75 from extraction, transport, processing of coal, oil and natural gas)(IEA, 2022). Although it is
76 important to tackle all sources of CH₄, emission reductions in the oil and gas (O&G) sector are
77 considered attractive, no-regret solutions. The International Energy Agency (IEA) estimates
78 that 75% of emissions reductions from the energy sector can be achieved at no net monetary
79 cost and could even result in economic savings, given that CH₄ is the main component of
80 natural gas and has commercial value (IEA, 2022). Thus, reducing CH₄ emissions from O&G
81 operations is one of the most substantial, easily accessible, and affordable mitigation actions
82 governments can take to address climate change.

83 Recent measurement-based studies in O&G production regions, mostly in North America,
84 have consistently shown that across years, scales, and methods, estimates of O&G CH₄
85 emissions often exceed emission inventory estimates (Zavala-Araiza et al. 2015; Shen et al.
86 2021; Gorchoy Negron et al. 2020; Robertson et al. 2020; Alvarez et al. 2018; Tyner and
87 Johnson 2021; MacKay et al. 2021) with a few exceptions (e.g. Yacovitch et al. 2018; Foulds et
88 al. 2022). Inventory estimates tend to be based on outdated generic emission factors, which
89 may not reflect actual technologies and practices. Also, counts and location of facilities and
90 equipment used in inventories may be inaccurate or incomplete. Lastly, current inventories do
91 not capture the statistical characteristics of emission distributions that are found across the
92 O&G supply chain, which are usually heavy tailed and positively skewed (Alvarez et al., 2018;
93 Zavala-Araiza et al., 2017).

94 Romania is one of the oldest O&G producers in Europe with the first exploration dating
95 back to 1857. In 2021, Romania was the second largest oil producer and natural gas producer
96 in the EU (BP, 2022). The recent gas discoveries in the Black Sea have the potential to hold
97 significant natural gas reserves, presenting an opportunity for the country to enter a new
98 phase of development. The EU announced an ambitious plan to urgently tackle CH₄ emissions
99 across all sectors by 2030 under the EU Methane Strategy (European Commission, 2020).
100 Underpinning this strategy, the EU recently announced draft regulations for the oil and gas
101 sector, focusing on robust measurement reporting and verification, leak detection and repair,
102 as well as minimizing venting and flaring (European Commission, 2021). In the case of
103 Romania, the uncertainty in current emission estimates and the lack of empirical data makes
104 the implementation of methane mitigation strategies challenging.

105 The Romanian Methane Emissions from Oil & Gas (ROMEIO) project aimed to address this
106 gap of knowledge (Röckmann, 2020). From September 30th to October 20th, 2019, a
107 measurement campaign took place in southern Romania with up to 70 participants from 14
108 research institutes. The goal of this project was to characterize CH₄ emissions at a component,
109 facility and basin scale using a variety of measurement platforms e.g., vehicles, Unmanned
110 Aerial Vehicles (UAVs), or commonly referred to as drones, and manned aircrafts. Through the
111 use of a range of emission quantification methods, the ROMEIO campaign aimed to provide a
112 comprehensive quantification of CH₄ emissions related to onshore O&G production in
113 Romania.

114 In this paper we analyse, integrate, and synthesize CH₄ emissions estimates collected by
115 vehicles and UAVs during the ROMEIO campaign, mainly focused on the characterization of oil
116 production sites. We (i) provide a comprehensive overview of the aggregated ground and
117 drone-based CH₄ emissions data, (ii) characterize the emission distributions and discuss the
118 differences between the quantification methods, (iii) present estimated emission factors
119 derived from the ground and drone-based measurements, (iv) identify major equipment
120 components of detected emissions across the O&G production sector, and (v) compare these
121 results to CH₄ emissions from emission inventories and production sites across other regions.

122 **2. Materials and methods**

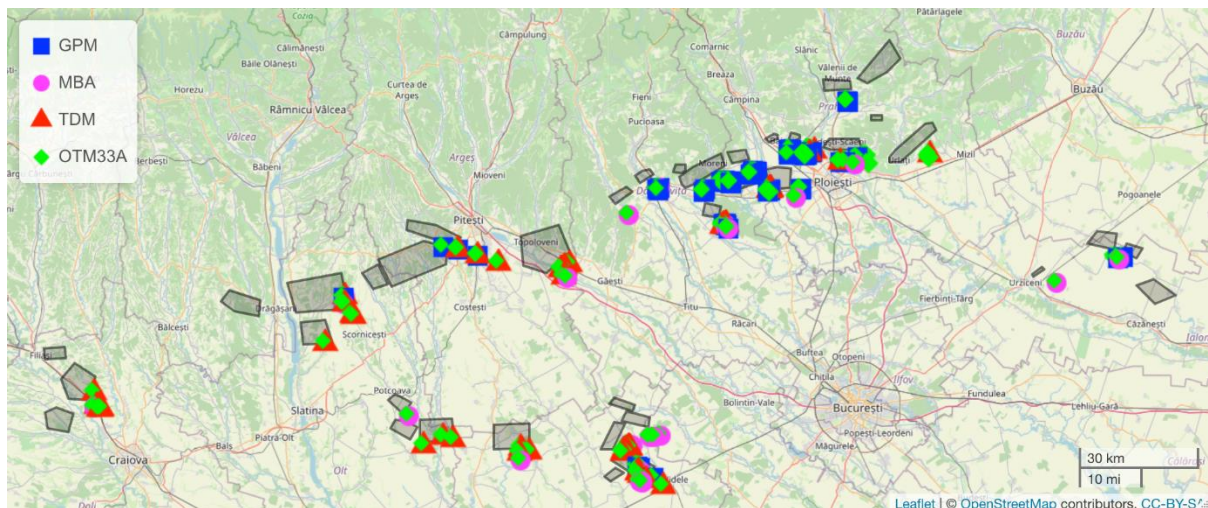
123 **2.1. Investigated area**

124 The 2019 ROMEIO campaign covered the southern part of Romania around the cities
125 Bucharest, Ploiesti, Pitesti, Targoviste and Craiova. Figure 1 shows that the O&G production
126 infrastructure is concentrated in smaller clusters that cover areas between 2 and 120 km²,
127 each containing 10 to 582 oil and gas related sites such as oil wells, gas wells, compressor
128 stations and oil parks. Different measurement teams visited different sites and clusters in
129 order to quantify as many O&G production sites as possible and to avoid a spatial sampling
130 bias. We note that most of the measurements presented here were individually described and
131 discussed in Delre et al. (2022) and Korbeń et al. (2022). Here we add the measurements
132 carried out from Unmanned Aerial Vehicle (UAV) platforms and integrate all ground and
133 drone-based data to perform upscaling emissions to the national scale.

134 The largest operator of O&G infrastructure in southern Romania, OMV-Petrom, provided a
135 list of production infrastructure coordinates and auxiliary information, such as type of
136 equipment, age, and for selected sites also production rate. Using this information, we
137 assessed the representativeness of our sampled sites in terms of production and age
138 characteristics (see S13 of Supplementary Material). A few additional emission points were
139 found that were not included in the infrastructure list provided by the operator. In these cases,

140 the site type was assigned based on visual inspection; in some cases, it could not be identified.
141 In our analysis we will combine the quantifications from all regions.

142 The majority of Romania's oil reservoirs are located in the southern part of the country.
143 With Romania producing about 3.3 million tonnes of oil in 2021 (BP, 2022), the southern region
144 is the most important part of the country's oil production sector. Most measurements during
145 the ROMEO campaign were collected from oil production sites, hence our analysis will focus
146 on this specific subset of sites. The oil production sites included in the study were usually
147 relatively simple, consisting of pump jacks and additional production equipment.
148



149
150 Figure 1. Map of the oil production sites that were quantified with four different measurement
151 approaches during the ROMEO campaign. The different symbols distinguish the different
152 quantification methods. Blue squares: Gaussian Plume Method (GPM); pink circles: Mass Balance
153 Approach (MBA); red triangles: Tracer Dispersion Method (TDM); green diamonds: Other Test
154 Method (OTM) - 33A. The grey shaded areas indicate clusters with high density of production facilities
155 (number of facilities ranging between 10 to 582), in some cases the symbols hide the areas.

156 2.2. Emission quantification

157 Facility scale measurements were divided into two phases: screening and quantification.
158 During the screening phase, the vehicles drove from site to site, circling the target site if
159 possible and recording CH₄ mole fractions above background. Screenings were performed
160 from public roads and the goal was to identify potential emissions at the site and check site
161 accessibility, considering factors such as roads condition, time limitations, and local
162 restrictions imposed by operators. To prevent any potential bias in the measured emissions,
163 the operators were not informed in advance about our visit to the facility, resulting in
164 occasional restricted site access. Additionally, the screenings aimed to determine whether off-
165 site sources such as other O&G infrastructure and farms, could interfere with subsequent
166 emission quantification, thereby ensuring the proper implementation of the quantification
167 methods. Also, a simplified Gaussian plume algorithm was applied for all locations where mole
168 fraction enhancements were observed to locate the sources based on the list of production
169 infrastructure provided by the operator, and to determine normalized CH₄ enhancements (see
170 S10 of Supplementary Material). A total of 1043 sites were screened using five cars. 85% of
171 these sites were oil production sites, and we focus on these for the following evaluation.

172 For quantification of CH₄ emission rates, four methods were used, namely the Tracer
173 Dispersion Method (TDM), Other Test Method (OTM) - 33A, Gaussian Plume Modelling (GPM)

174 using plume measurements from vehicles and Mass Balance Method (MBA) using Unmanned
175 Aerial Vehicle (UAV) based measurements (see S1). Here we provide a brief description of each
176 measurement method. Delre et al. (2022) provides additional information on the deployment
177 of TDM and GPM during the ROMEO campaign, while Korbeń et al. (2022) offers details
178 specifically on the deployment of OTM-33A and GPM.

179 The Tracer gas Dispersion Method (TDM) or tracer release method (Lamb et al. 1995) has
180 been widely used to quantify CH₄ emissions in the O&G sector (Allen et al., 2013; Zavala-Araiza
181 et al., 2018; Yacovitch et al., 2017; Roscioli et al., 2015). TDM involves the release of a tracer
182 gas at a controlled rate. When the tracer gas is released close to an emission point of the target
183 gas (CH₄), both gases undergo the same atmospheric transport processes. Therefore, even
184 when the plume dilutes, the ratio of their observed enhancements remains the same as the
185 ratio of their emission rates. Atmospheric concentrations of both the target gas and the tracer
186 gas can then be measured downwind to determine the unknown emission rate of the target
187 gas (CH₄). In this study, acetylene (C₂H₂) and nitrous oxide (N₂O) were used as tracer gases.

188 Two vehicles equipped with laser gas analysers were used to quantify CH₄ emissions with
189 the TDM. The first vehicle was equipped with two cavity ring-down spectroscopy analysers.
190 One instrument measured CH₄ (G2401, Picarro, Inc., Santa Clara, CA), and the other one
191 measured acetylene (C₂H₂) and nitrous oxide (N₂O) (S/N JADS2001, Picarro, Inc., Santa Clara,
192 CA). The second vehicle used a dual laser trace gas monitor based on Tunable Infrared Laser
193 Direct Absorption Spectroscopy to detect CH₄, C₂H₆, N₂O, CO₂, and CO simultaneously
194 (Aerodyne Research Inc., Billerica, MA). Measurements of CH₄ and tracer gases concentrations
195 were carried out by performing on average 9 downwind plume traverses. The site-
196 representative methane emission rate was then calculated by averaging the emission rates
197 estimated from the multiple traverses across the plume. A total of 50 quantifications were
198 performed at different sites using mobile and, in a few cases, static TDM.

199 The Gaussian plume method (GPM) uses an idealized calculation for the average local-scale
200 CH₄ dispersion, assuming constant meteorological conditions in time and space over a flat
201 region, to derive emission rate estimates from plume observations (Hanna et al. 1982). The
202 emission rate can then be calculated from measurements downwind of a source, using
203 information about the height of the source, wind speed and wind dispersion parameters
204 (Riddick et al., 2017). During the ROMEO campaign, multiple cars transects were carried out
205 downwind from the source at locations suitable for GPM. The emission rate for each location
206 was estimated based on the comparison between the results of the actual measured
207 concentrations and the results of the GPM. A total of 111 measurements were performed at
208 a variety of sites using GPM. GPM sub-sets from ROMEO have been investigated in Delre et al.
209 (2022) and Korbeń et al. (2022). In our analysis, we combine the GPM evaluation from the
210 different teams into one subset of emission quantifications.

211 Delre et al. (2022) compared emission rates derived from TDM and GPM evaluation
212 methods at 41 O&G sites. They found lower estimates from GPM evaluations compared to
213 TDM and applied a correction of a factor of 2 or more to the GPM quantifications (Delre et al.,
214 2022). We do not apply a correction to GPM measurements as done in Delre et al. (2022),
215 since a comparison to TDM is not possible for the other measurement teams (Korbeń et al.,
216 2022). Including the correction would lead to higher emission rate estimates. We also use a
217 different (parametric) statistical evaluation as described below.

218 Other Test Method (OTM) 33A is one of the Geospatial Measurement of Air Pollution
219 Remote Emission Quantification (GMAP-REQ) approaches developed by the United States
220 Environmental Protection Agency (EPA) (Thoma and Squier, 2014). This method uses
221 measurements with stationary analysers to detect and quantify emissions from a variety of

222 sources located near-field and at ground level (Robertson et al., 2020). Measurements were
223 performed by two vehicles equipped with in situ CH₄ analyzers. The first vehicle was equipped
224 with a high-precision Optical Feedback—Cavity-Enhanced Absorption Spectroscopy analyzer
225 (Licor Li-7810, LI-COR, Inc.) and detected CH₄ and CO₂ concentrations in ambient air. The
226 second vehicle was equipped with a cavity ring down spectrometer (CRDS, Model G1301,
227 Picarro Inc.). A total of 77 quantifications were performed at different sites using OTM-33A.

228 The Mass Balance Approach (MBA) has been applied widely to aircraft-based
229 measurements of CH₄ and other trace gases from the facility scale up to the basin scale (Karion
230 et al., 2013; O’Shea et al., 2014; Baray et al., 2018; Pitt et al., 2019). This method involves flying
231 at multiple heights downwind and/or around a region containing a possible emitting source
232 and measuring trace gas concentration and wind speed. Emission rates of the net surface flux
233 within that volume are then estimated from the difference between downwind and upwind
234 measurements (Morales et al., 2022).

235 Unmanned Aerial Vehicles (UAVs) are an emerging platform to investigate CH₄ emissions
236 from various sources such as landfills, dairy farms and natural gas compressor stations (Allen
237 et al., 2019; Vinković et al., 2022; Nathan et al., 2015; Andersen et al., 2018; Morales et al.,
238 2022; Shah et al., 2020; Shi et al., 2022). UAVs allow transecting the plume over its entire
239 vertical and horizontal extent, by flying at numerous heights, compared to ground-based
240 measurements that typically capture only part of the plume only at one height (Andersen et
241 al., 2018). Two different UAV-based systems were used to obtain atmospheric mole fraction
242 measurements downwind of oil and gas facilities during ROMEO: (i) an active AirCore system
243 from the University of Groningen (UG) (Vinković et al. 2022) and (ii) a lightweight fast-response
244 Quantum Cascade Laser Absorption Spectrometer (QCLAS) developed at the Swiss Federal
245 Institute for Materials Science and Technology (EMPA) (Tuzson et al., 2020; Morales et al.,
246 2022). A total of 125 flights (65 UG; 60 EMPA) were performed downwind of 43 different
247 facilities (19 UG; 24 EMPA). Both UAV-based techniques use an MBA to quantify the emission
248 rates from sampled oil and gas facilities, but there are certain differences in the MBA between
249 UG and EMPA application, including factors such as the treatment of wind, which are
250 presented in the supplementary material.

251 Several studies of CH₄ emissions from O&G infrastructure have found that emissions
252 distributions are typically heavy tailed and positively skewed with a small fraction of sites (i.e.,
253 super-emitters) accounting for a disproportionate fraction of emissions. These distributions
254 often become symmetric and normal when plotted as the logarithm of emissions. To account
255 for this behaviour, lognormal distributions have been widely used in the literature to more
256 accurately characterize emissions (Alvarez et al. 2018; Zavala-Araiza et al. 2015; 2017; 2018;
257 Robertson et al. 2020; Omara et al. 2016; Brandt et al. 2016; Yacovitch et al. 2017). We
258 examine whether our sampled data with emissions from oil production sites follow a
259 lognormal distribution by using two statistical tests (see S3). Table S2 of the supplemental
260 material shows that the null hypothesis of lognormality is accepted by both the Shapiro-Wilk
261 and Lilliefors test for all four measurement methods.

262 Several studies have evaluated site-level measurements from the O&G infrastructure using
263 non-parametric bootstrapping methods to derive emission factors (Rella et al., 2015; Brantley
264 et al., 2014; Robertson et al., 2017; Omara et al., 2016; Riddick et al., 2019). The previous
265 publications that evaluated subsets of the measurements reported here (Delre et al., 2022;
266 Korbeń et al., 2022) also used non-parametric approaches to estimate emission factors for a
267 systematic literature comparison. Non-parametric approaches typically derive EFs significantly
268 lower than the ones using parametric approaches. The parametric approaches take into
269 account the skewed distribution of the emission rates, particularly the disproportionate

270 contribution of emissions from the heavy tail of emission distributions. In particular, they
271 include the possibility that in the full distribution of sites, emission rates exist which are above
272 the maximum of the sampled subset. Therefore, parametric approaches and log-normal fits
273 have been used for up-scaling (Alvarez et al., 2018; Zavala-Araiza et al., 2015; Robertson et al.,
274 2020). As the emissions distribution in this work is highly positively skewed (see below), we
275 apply the parametric approach for scaling up to the total population of oil production sites in
276 Romania.

277 To this end, we calculate probability density functions (pdfs) of measured emission rates
278 that follow a log-normal distribution using Maximum Likelihood Estimation (MLE) (Zavala-
279 Araiza et al., 2015, 2018; Alvarez et al., 2018; Robertson et al., 2020). These pdfs are then used
280 to derive representative site-level Emission Factors (EF) which consider the low probability of
281 high-emission sites that describe skewed distributions. The mathematical formalism of this
282 statistical estimator is described in section S4 of the supplementary material, and we refer to
283 this approach as our reference method (A1).

284 The implementation of the log-normal fits requires information about the detection limit
285 of each method and the number of sites with emissions below this value (referred to as *non-*
286 *detects*). However, even when using the same analytical platform to measure emissions, the
287 lowest detectable emission rate will be affected by the distance between the emission point
288 and the analyser and by the meteorological conditions for a given measurement (Delre et al.,
289 2017). For our analysis, the detection limit for OTM-33A, GPM and MBA was empirically
290 determined equal to 0.11 kg h^{-1} and for TDM equal to 0.07 kg h^{-1} . Delre et al. (2022) and Korbeň
291 et al. (2022) determined the fraction of sites with emission rates below these detection limits
292 as 27% for TDM and 35% for OTM-33A, and GPM; the latter value is also adopted for MBA.

293 On the component scale, the combination of an Optical Gas Imaging (OGI) camera for the
294 detection of potential leak sources and a Hi-Flow Sampler (HFS) device for the quantification
295 of the emissions was implemented. A total number of 181 sites including 155 oil production
296 sites were visited and screened with a Forward-Looking InfraRed (FLIR) GasFindIR infrared
297 camera, the majority of them from the fence line. 231 individual leaks were detected with the
298 OGI camera but because of limited site access, the emission rates of only 62 leaking
299 components were measured using the HFS method. IR videos of the leaking components were
300 recorded to document detected emissions. These videos were reviewed to verify the number
301 of emission points and identify the type of emitting equipment.

302 From the OGI surveys we determined that a small but significant fraction of sites had no
303 emissions. While these surveys could potentially miss sources of emissions since they were
304 performed from the fence line (vs on-site), it allows us to derive a more conservative site-level
305 estimate, where we only add 1/3 of the non-detects to the main distribution of emitters. The
306 other 2/3 of the non-detects are considered as a separate mode of non-emitters with an EF of
307 0. These sites will also not be considered in the upscaling (see below). The final parameters
308 that are considered for the determination of the emission rate are provided in Table 2. A
309 detailed discussion on the determination of non-detects and the detection limits of the
310 different techniques is provided in sections S5 of the supplementary material. The effect of
311 the fraction of non-detects and the detection limit on the log-normal fits and the final EFs is
312 further explored by testing several different values (section S5). We find that reducing the
313 detection limit or increasing the fraction of non-detects leads to higher estimated EFs due to
314 the widening of the distribution towards the lower end. This emphasizes the importance and
315 need of conducting a thorough investigation when selecting the values for these two
316 parameters.

317 Additionally, in section S7 we present a sensitivity analysis with alternative upscaling
 318 approaches to explore upper and lower limits of the EF estimate for oil production sites. The
 319 main differences between these approaches are the choice of the detection limit and fraction
 320 of non-detects, the separation of the data into west and east regions and the separation by
 321 measurement method.

322 The combination of site-level emission estimates and component-level OGI surveys
 323 provided insights into the magnitude of emissions from oil production sites as well as key
 324 mitigation opportunities.

325

326 3. Results

327 3.1. Site-level quantifications of oil production sites

328 Approximately 887 oil production sites were screened, and emission rates were quantified
 329 from a total of 178 oil production sites. Table 1 provides basic statistics of the results obtained
 330 with the different measurement methods. The difference between the arithmetic mean and
 331 median estimates and the high positive values of skewness and kurtosis parameters
 332 demonstrate that the emission rates were positively skewed with a heavy tail for all methods.
 333 We find that the OTM-33A and GPM show the highest values of skewness and kurtosis,
 334 whereas the TDM and MBA present the least skewed and heavy tailed distributions. Figure 2
 335 illustrates the boxplots of the distributions of the quantified emission rates per method. It is
 336 important to note that the sampled oil production sites are different for each method (and
 337 sampled at different points in time), thus Figure 2 summarizes the sampled emissions
 338 distributions and the observed differences in Figure 2 may be influenced by factors such as
 339 variations in emissions magnitude and variability at each specific oil production site.

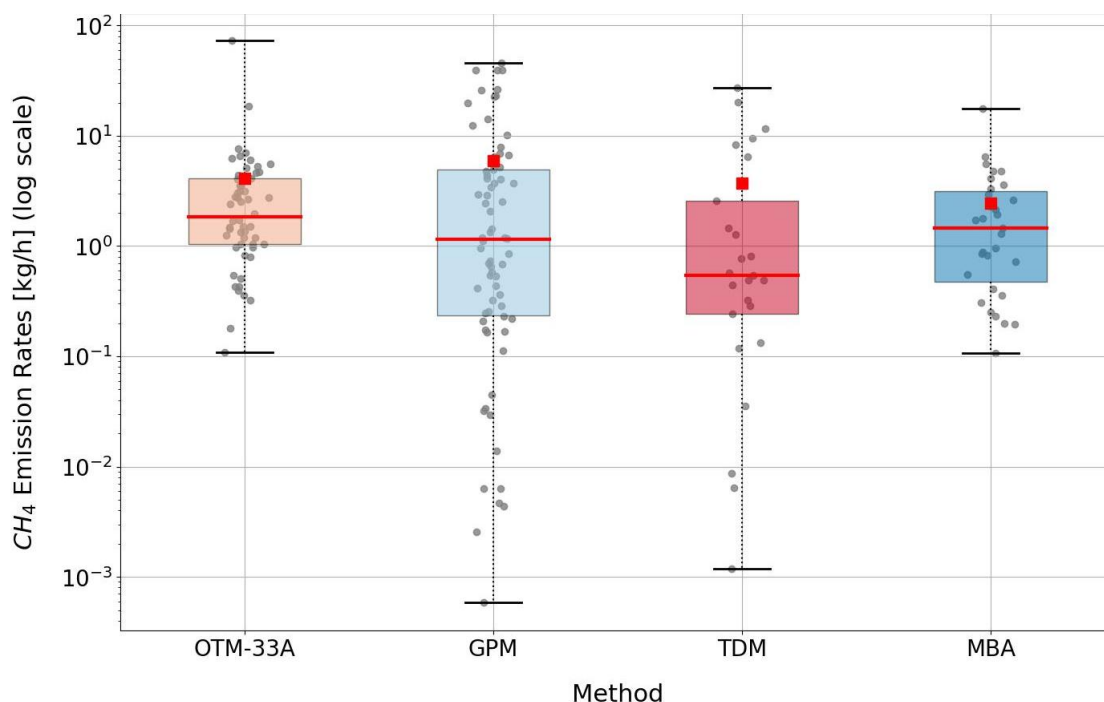
340 Table 1. Basic statistics of measured CH₄ emission rates by method.

Method	# Oil production sites	Arithmetic mean [kg h ⁻¹]	Median [kg h ⁻¹]	Min [kg h ⁻¹]	Max [kg h ⁻¹]	Skew ^b	Kurtosis ^c
OTM-33A	54	4.1	1.9	0.1100	73	6.3	40
GPM ^a	68	6.1	1.0	0.0006	118	5.4	34
TDM	25	3.7	0.5	0.0012	27	2.3	4
MBA	31	2.4	1.5	0.1100	18	3.3	12

341 ^aIncluding the oil production sites evaluated as "Estimate" in Delre et al. (2022) using only one
 342 concentration record (see S2)

343 ^bSkewness is a measure of the asymmetry of a data distribution. Skewness of zero represents a normal
 344 distribution. Positive (negative) values indicate that the data is positively (negatively) skewed.

345 ^cKurtosis is a measure indicating whether the data distribution is heavy-tailed or light-tailed relative to
 346 a normal distribution. Kurtosis of zero represents a normal distribution. Positive (negative) kurtosis
 347 indicates a "heavy-tailed" ("light-tailed") distribution.



348
 349 Figure 2. Boxplots of the distributions of quantified emission rates from oil production sites per
 350 method. In each box the red horizontal line signifies the median and the red squares show the mean.
 351 The box extends to the 25th and 75th percentiles. The whiskers extend from the minimum to the
 352 maximum value. The data points are overlaid on top of the boxplots (grey dots). Note the logarithmic
 353 y-axis.

354 3.2. Emissions distributions and emission factors

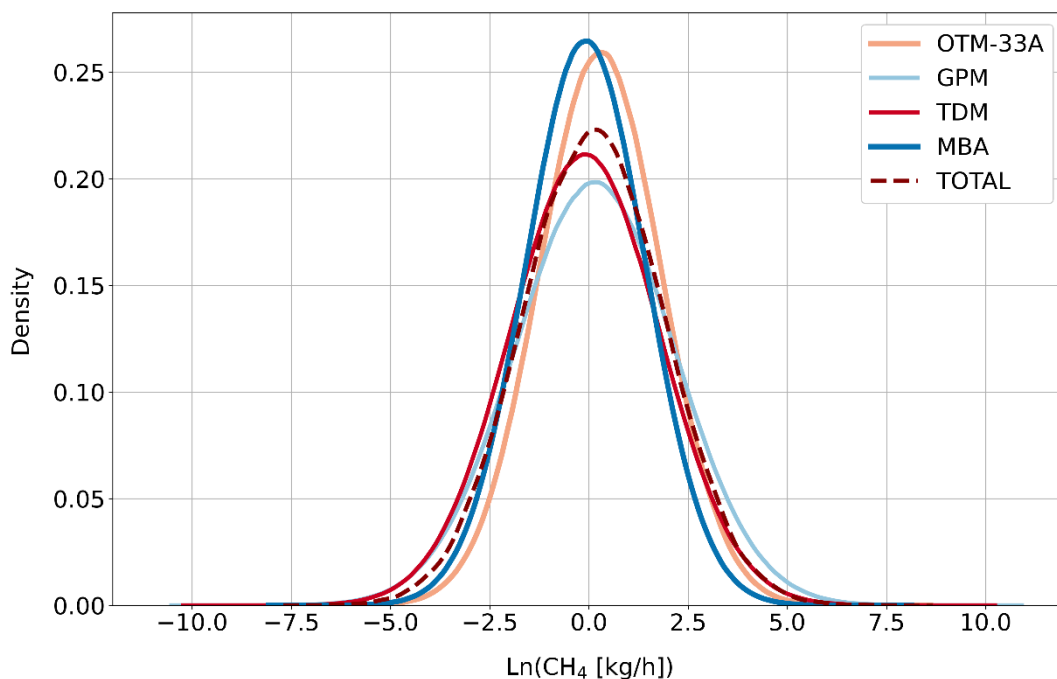
355 Figure 3 shows the pdfs generated from fitting the quantified emission rates to lognormal
 356 distributions. In Table 2 we summarize key parameters and derived EFs that characterize these
 357 distributions. Across methods, best estimates for EFs range from 2.9 – 8.8 kg h⁻¹ of CH₄ site⁻¹.
 358 The pdf of GPM shows the widest distribution and a large confidence interval (CI). The effect
 359 of the small sample size is reflected in the large 95% CI of TDM relative to the other methods.
 360 When we combine all the quantifications (solving for one single Maximum Likelihood
 361 Estimation, see SM) we obtain a central estimate of mean site-level emission equal to 5.4 kg
 362 h⁻¹ of CH₄ site⁻¹ (3.6 – 8.4, 95% CI). For information, histograms and fitted pdfs for each method
 363 used are shown in Fig. S7 of the SM.

364
 365 Table 2. Summary of parameters from the statistical estimator.

Method	DL [kg h ⁻¹]	S _r	S _o [% of non- detects]	μ	σ	EF [kg h ⁻¹ site ⁻¹]	95% CI
OTM-33A	0.11	53	7 [12%]	0.28	1.54	4.3	2.4 – 8.2
GPM	0.11	57	8 [12%]	0.15	2.01	8.8	3.7 – 23
TDM	0.07	21	2 [9%]	-0.10	1.89	5.4	1.6 – 23
MBA	0.11	30	4 [12%]	-0.08	1.51	2.9	1.4 – 6.6
TOTAL	-	-	-	0.12	1.77	5.4	3.6 – 8.4

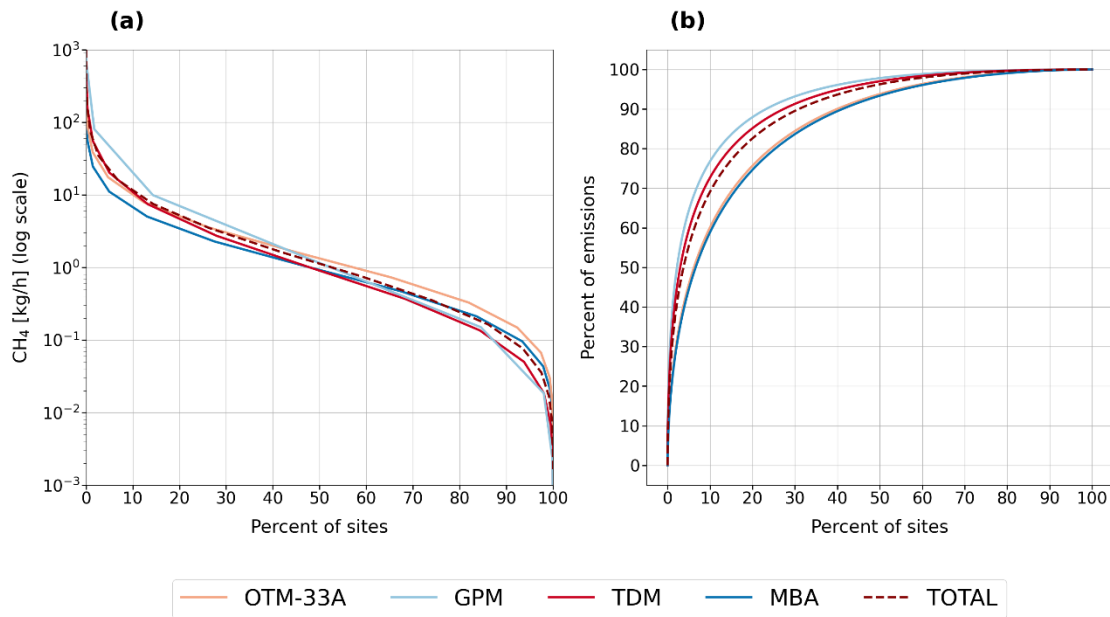
366 DL is the assigned detection limit for each measurement method, S_r is the number of measurements
 367 above the detection limit, S_o is the number of measurements at or below the detection limit (included
 368 as censored data). Note that in actual measurements even emission rates below this limit are

369 sometimes detected (see Fig. 2). In our statistical approach these measurements are replaced by the
 370 fraction of non-detects S_0 . Therefore, the numbers for S_r are different the total number of oil
 371 production sites visited given in Table 1. $EF = e^{\mu + \frac{1}{2}\sigma^2}$, TOTAL
 372 presents the results of the statistical estimator considering all four measurement methods.



373
 374 Figure 3. Fitted pdfs of the statistical estimator for each measurement method.

375 The cumulative distribution functions and Lorenz curves from all measurement methods
 376 using the statistical estimator (Fig. 4) verify once more that the distributions are highly skewed.
 377 For the quantified population of oil production sites, we find that 10% of emitters had
 378 emissions greater than 10 kg h^{-1} and were responsible for over 70% of total emissions. The
 379 estimates from the different methods reflect the qualitative illustration in Fig. 3: The results
 380 obtained with GPM show the most skewed distribution with the 10% of oil production sites
 381 with highest emissions contributing to 77% of total emissions, whereas for the oil production
 382 sites measured with the MBA 60% of cumulative CH_4 emissions are attributed to 10% of oil
 383 production sites.



384

385 Figure 4. a) Cumulative distribution functions, b) Lorenz curves: percent of emissions as a function
 386 of percent of sites. For both graphs, oil production sites are sorted from high to low emission rates
 387 (descending order).

388 In the supplementary material (sections S7) we provide additional estimates of the total
 389 CH₄ basin EFs calculated using modifications of the reference statistical approach in order to
 390 explore the sensitivity to the chosen parameters. By using the same reference approach and
 391 including a higher fraction non-detects, ranging between 27 – 35%, the derived EF is 53%
 392 higher. Compared to the EF calculated with the reference approach, the EFs calculated using
 393 the alternative approaches are between 35 –83% higher. All of these estimates agree within
 394 the ranges of uncertainty, confirming that the high EFs are not due to details of the statistical
 395 treatment. For comparison of our values to other studies (see below) we use the Ref scenario
 396 (A1) discussed in the previous sections which is our lowest and most conservative estimate
 397 and includes a separate mode of non-emitters (zero mode) and a correspondingly lower
 398 fraction of non-detects for the main mode of emitters (9 - 12%).

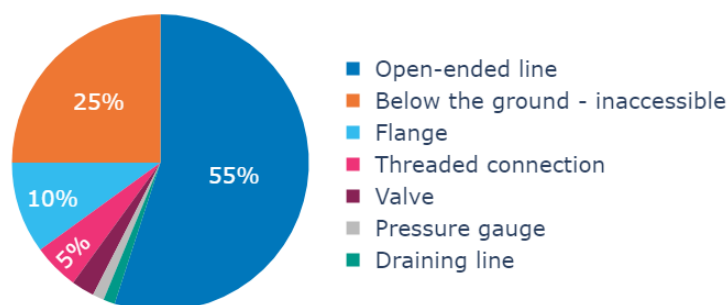
399

400 3.3. Identification of leaking components

401 By using the recorded videos of the leaking components, emission sources could be
 402 attributed to specific major equipment types across the O&G production sector. A total of 155
 403 oil production sites were screened with the infrared camera, corresponding to approximately
 404 3% of the total population of oil production sites provided by the operator. CH₄ emissions were
 405 detected from approximately half (49%) of these sites. At least one leak was detected at 74
 406 out of the 155 screened oil production sites with an average of 1.2 leaks detected per site. A
 407 total of 86 individual leaks were identified at the oil production sites. The HFS method was
 408 used to measure emissions from a small subset of leaks (i.e., when access to the leaky
 409 component was possible), results are summarized in the SM (see S11) but were not used as
 410 part of the main analysis since they do not represent a complete assessment of the magnitude
 411 of emissions.

412 Figure 5 shows the distribution of the identified leaking components for oil production
 413 sites. The most frequently detected sources were open-ended lines, accounting for more than
 414 half (55%) of the detected components. An open-ended line refers to a pipe or tubing that is

415 not sealed at one end, and therefore remains open to the atmosphere, allowing all gas to be
 416 vented to the atmosphere. Following open-ended lines, inaccessible components located
 417 below the ground comprised 25% of the detected sources, while malfunctioning equipment
 418 such as flanges and threaded connections accounted for 20%. It should be noted that the
 419 inaccessible and, as a result, non-identified components below the ground may consist of
 420 valves, pumps, connectors, or potentially open-ended lines.



421

422 Figure 5. Frequency of identified leaking components for oil production sites (n = 86).
 423

424

3.4. Other types of facilities

425 In addition to oil production sites, we visited also other types of infrastructure (gas
 426 production sites, oil parks, compressor stations, etc) during the ROME campaign. Due to the
 427 low number of quantifications for these types of infrastructure, a statistically robust
 428 quantitative evaluation is impossible, but we provide here some qualitative information. The
 429 largest emission rates were observed from an oil park with 138 kg/h, while the average
 430 emission rate from 17 oil parks was 17 kg/h. An oil park is a facility designed to gather, store,
 431 and distribute oil produced from multiple individual wells in the surrounding area. The most
 432 important sources of CH₄ emissions from oil parks were leaks in storage tanks and other
 433 malfunctioning equipment, such as valves or flanges. We visited two compressor stations and
 434 found 58 and 27 leaks, approximately half of them were quickly repaired in one day by the
 435 technicians from the operator. The complete list of all quantifications is provided in section
 436 S14 of the SM.

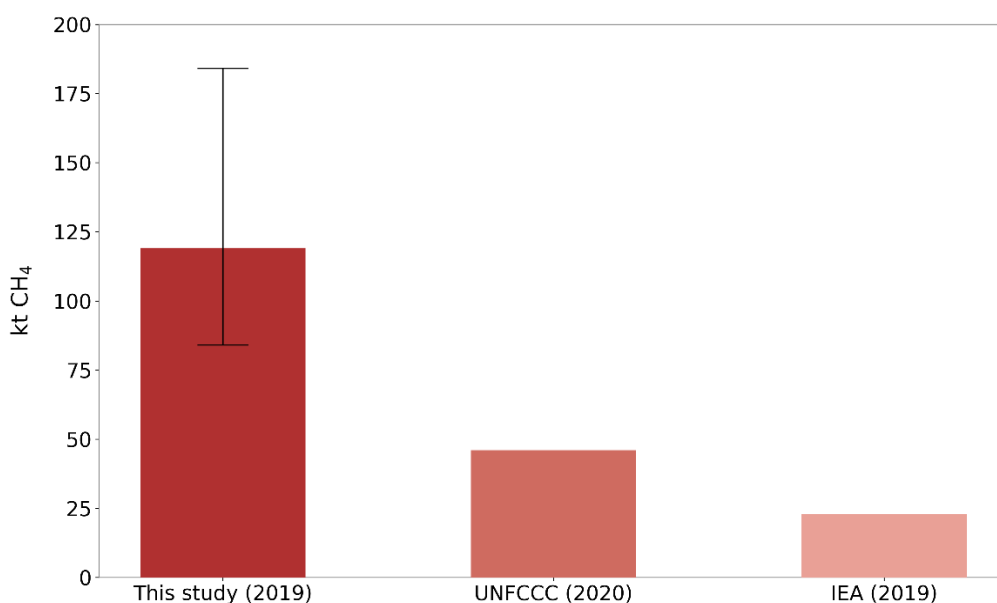
4. Discussion

437
 438 To compare our results with the reported emissions from national inventories, we assume
 439 that the measured oil production sites in this study are representative of oil production sites
 440 basin-wide. We scale up our emissions to the country level by using our central estimate of
 441 5.4 kg h⁻¹ site⁻¹ for the evaluation including a separate mode of no-emitters, as explained
 442 above. This leads to an activity factor of N ≈ 2500 for the year 2019. Assuming that these
 443 emissions continue year-round, this results in annual emission estimate of 120 ktons CH₄ (min
 444 = 79 ktons and max = 180 ktons, 95% CI).

445 In Fig. 6, our measurement-based estimates are compared to inventory reports. Methane
 446 emissions from Romania for the year 2020 reported to the United Nations Framework
 447 Convention on Climate Change (UNFCCC) in category 1.B.2.a (CH₄ from Oil, sub-categories i:
 448 exploration and ii: production) and category 1.B.2.c (Venting and Flaring) sum up to 46 ktons
 449 of CH₄ (Greenhouse Gas Inventory Data - Comparison by Category, 2022). The IEA estimate for

450 Romanian emissions from the categories *Onshore Oil* and *Other from oil and gas* for the year
 451 2019 is 23 ktons of CH₄ (Methane Tracker Data Explorer, 2022). Thus, the emission rates
 452 derived in our study are approximately 2.5 times higher than the UNFCCC inventory and more
 453 than 5 times higher than the IEA estimate. Note that our reference statistical approach is a
 454 conservative one as shown in the sensitivity study in the SM. Our estimates also only include
 455 producing oil production sites, and not even the total population of oil production sites in
 456 Romania. Documented emissions from other types of sites, e.g., oil parks with our
 457 documented emissions from leaking tanks, and the entire gas production infrastructure, were
 458 not included. Non-producing oil production sites were also neglected for the derivation of
 459 country-level annual emissions, although emissions were still detected from nine oil
 460 production sites that were characterised as non-operating by the operator.

461 The total emission rate from all oil production sites that were quantified in this study was
 462 810 kg/h whereas the sum of quantifications of all types of infrastructure visited during the
 463 ROMEO campaign was 2100 kg/h. Although we do not have a sufficient statistical basis for a
 464 thorough quantification of other types of infrastructure, this indicates that the total CH₄
 465 emissions from the O&G infrastructure in Romania could be at least a factor 2 higher than our
 466 estimate from oil production sites.



467 Figure 6. Comparison of annual CH₄ emissions estimated in our study for 2019 with emissions
 468 reported to the UNFCCC in category 1.B.2.a (CH₄ from Oil, sub-categories *i*: exploration and *ii*:
 469 production) and category 1.B.2.c (Venting and Flaring) for the year 2020 and derived by the IEA for
 470 categories *Onshore Oil* and *Other from oil and gas* for the year 2019. Error bar extends from the lower
 471 bound (i.e., 79 ktons yr⁻¹) to the upper bound (i.e., 180 ktons yr⁻¹) of the 95% CI.
 472

473 Discrepancies between available inventory estimates and direct measured CH₄ emissions
 474 have been indicated by numerous studies in other areas (Robertson et al., 2020; MacKay et
 475 al., 2021; Alvarez et al., 2018; Zavala-Araiza et al., 2015; Tyner and Johnson, 2021; Rutherford
 476 et al., 2021), and we now confirm this discrepancy is large for Romania. One reason for these
 477 discrepancies is the use of outdated and highly uncertain EFs for the derivation of inventory
 478 estimates. This is especially relevant for Romania since their published estimates are based on
 479 the basic Tier 1 method, which relies on multiplying default EF applicable for all countries by

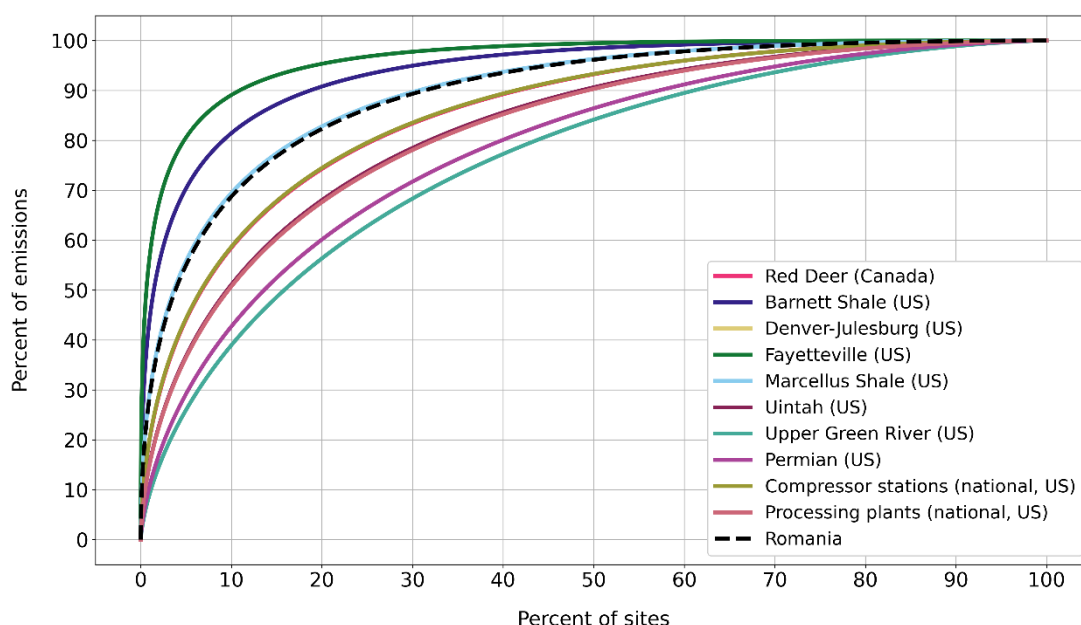
480 country-specific activity data following the IPCC 2006 guidelines (Eggleston et al., 2006). Thus,
 481 these reported emissions do not consider the characteristics of the actual O&G infrastructure
 482 of Romania, such as its age and state of maintenance, or current operational practises. For
 483 example, emission reduction by gas flaring has been almost eliminated as a practice in
 484 Romania. Additionally, infrastructure for the collection and economical utilization of the
 485 natural gas that would otherwise be flared or vented is inadequate or non-existing in the
 486 sampled areas, as illustrated by the high fraction of surveyed sites, where direct venting was
 487 the main source of emission.

488 To place the results from the ROMEO campaign in perspective, we compare them to studies
 489 performed in O&G production areas in the US and Canada (Robertson et al., 2020, 2017;
 490 Zavala-Araiza et al., 2015, 2018; Omara et al., 2016). We use the reported datasets from these
 491 studies to derive the EFs using the statistical approach used in this paper. In this way we
 492 eliminate inconsistencies from data treatment and can consistently compare the results
 493 between the different regions.

494 The CH₄ EF estimated for Romania is 5.4 kg h⁻¹ site⁻¹ (3.6 – 8.4, 95% CI). EFs estimated for
 495 the studies used for our comparison range between 1.2 and 8.2 kg h⁻¹ site⁻¹ for O&G
 496 production sites (e.g., oil well and/or gas well sites), with the majority of the EFs being below
 497 3 kg h⁻¹ site⁻¹ (see Table S13). Specifically, our estimated CH₄ EF from Romania is the third
 498 highest EF calculated from a variety of production regions in North America. The differences
 499 between production characteristics, age of sites, geologic features and operational procedures
 500 in each region could have a significant impact on the various levels of skewness and the EFs.

501 Figure 7 shows the derived cumulative distribution functions of each production region. All
 502 studies show heavy-tailed distributions; however, Romania presents the fourth highest level
 503 of skewness indicating the disproportionate contribution of high-emitting sites to the total
 504 emissions. Our results show that 10% of sites are responsible for more than 70% of emissions.
 505 By identifying and mitigating these high-emitting sites or "super-emitters", a large share of
 506 total emissions reduction can be achieved.

507

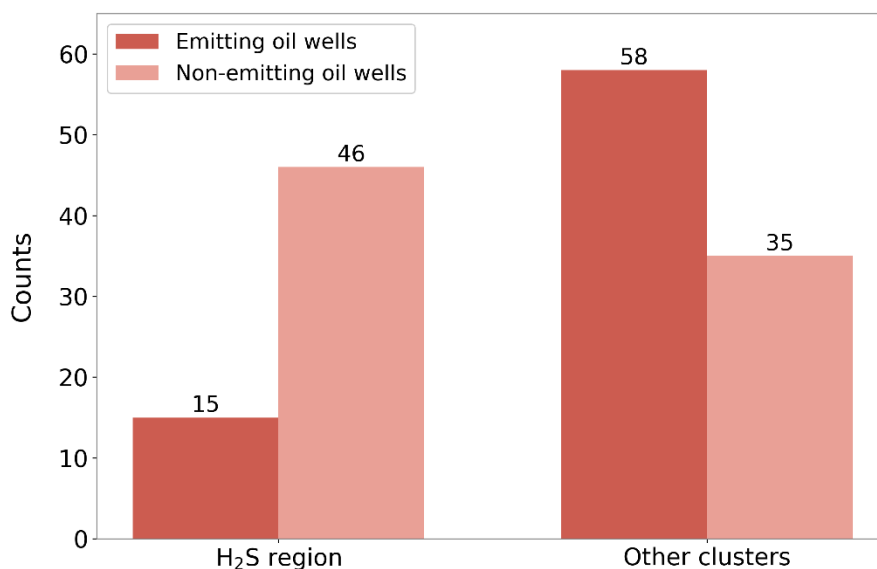


508
 509 Figure 7. Lorenz curve: cumulative percentage of emissions as a function of cumulative percentage of
 510 sites (sorted from high to low emissions) for different North American production regions, including
 511 the results from this study. The black dashed line shows the results of the statistical estimator for the

512 ROMEO campaign, considering all four measurement methods. It overlaps with the one from the
513 Marcellus Shale basin. Red deer line overlaps with compressor stations line, and Uintah line overlaps
514 with processing plants line.

515 On the component scale, 55% of emission points from oil production sites are from open-
516 ended lines and another 25% from non-identified components below the ground, which are
517 possibly open outlets as well. These vents are thus part of the operational practices and can
518 be avoided by prioritizing gas capture infrastructure.

519 An important finding of the OGI dataset analysis is the much lower percentage of emitting
520 oil production sites in a production cluster, where the produced oil is associated with
521 emissions of Hydrogen Sulfide (H₂S) gas (Fig. 8). H₂S is a by-product that is formed in some
522 fossil fuel reservoirs through natural processes or due to some methods employed in the O&G
523 upstream production (Marriott et al., 2016). It is highly toxic to humans and animals, causing
524 serious health problems even at low concentrations (Doujaiji and Al, 2010). The lower fraction
525 of emitting oil production sites in this cluster indicates that sites associated with the H₂S
526 component are better maintained to avoid harmful H₂S emissions. This demonstrates that it
527 is feasible to reduce emissions by improved practises and better maintenance of facilities.
528 These findings are consistent with the research conducted by Lavoie et al. (2022), which
529 showed that reduction strategies focusing on olfactory compounds in Peace River have proven
530 beneficial in reducing and maintaining lower CH₄ emissions, despite not being specifically
531 designed for CH₄ reduction purposes (Lavoie et al., 2022). However, it is important to note
532 that further research is needed to establish a clear relationship between CH₄ and H₂S emission
533 rates.



534 Figure 8. Number of screened oil production sites, divided by sites with identified leaks and sites
535 without identified leaks, from the H₂S region in comparison to other clusters.
536

537 An independent line of evidence for large scale venting in Romania is that 70% of the
538 screened oil production sites and more than 50% of measured oil production sites are listed
539 with zero gas production in the database of the operator. Evidently, when associated gas is
540 vented via open vents immediately at the well head, it will not be metered and thus cannot
541 be quantified and reported.

542 Our results have great implications not only for the accuracy of current national inventories,
543 but also for the feasibility of reaching EU emissions reductions targets. The total CH₄ emissions
544 from the O&G sector in Romania reported to the UNFCCC decreased by 93% between 1989
545 and 2020 (Greenhouse Gas Inventory Data - Comparison by Category, 2022). However, this
546 significant reduction is primarily due to the change of the TIER 1 emission factor from the one
547 for developing countries to the one for developed countries in the year 2000. It is a
548 consequence of decrease in production and changes in reporting methodology, and not
549 indicative of changes in operations that would result in lower emissions. The lack of gas flaring
550 and gas collection infrastructure across oil production sites in Romania is evidence of the
551 relatively high emissions. Additionally, a large number of countries rely on the Tier 1 method,
552 rather than direct site-level measurements, for the derivation of their national emissions
553 estimates from the energy sector. However, since technological and operating conditions vary
554 significantly between countries, these estimates are associated with large uncertainties and
555 might not reflect actual emissions.

556 Our work highlights the need for better understanding of the level of emissions in the O&G
557 industry. Due to the significant regional differences in age, site design, and operational
558 practices, the O&G production region in one country, such as southern Romania, may not be
559 representative of other production regions around the world. Therefore, emission factor
560 estimates, and mitigation options cannot be generalised. Our work, however, illustrates how
561 empirical data collected at both facility and component scales can significantly reduce the
562 uncertainty in the magnitude of emissions and identify key mitigation opportunities specific
563 to a country's local conditions.

564

565 **5. Conclusions**

566 In this work, we provide a thorough characterization of CH₄ emissions from oil production
567 sites in Romania by integrating a variety of ground and drone-based quantification methods.
568 The main findings are summarized as follows:

- 569 1. Emission rates from oil production sites were represented by a mean EF equal to 5.4 kg
570 h⁻¹ site⁻¹ (3.6—8.4, 95% CI). The derived EF for Romania is one of the highest EFs found
571 in previous studies.
- 572 2. The CH₄ emission rate distribution is highly skewed, with 10% of sites contributing to
573 more than 70% of the total CH₄ emissions.
- 574 3. Oil production sites associated with emissions of H₂S are better maintained and had a
575 lower number of detected emission points compared to oil production sites without H₂S
576 emissions. Thus, effective mitigation of emissions can be achieved by improved practices.
- 577 4. The Romanian national inventory underestimates O&G CH₄ emissions by at least a factor
578 of 2, likely more. Given the importance of mitigating CH₄ emissions in the near-term
579 future, and the ambitious mitigation targets announced by governments and industry,
580 improvement of emission reporting based on measurements is key to track changes in
581 emissions over time.
- 582 5. Major drivers of CH₄ emissions from oil production sites in Romania are the venting of
583 gas through open-ended lines followed by technical malfunctioning equipment.
- 584 6. Our results highlight significant opportunities for emission mitigation. Development of
585 infrastructure for the capture and utilization of natural gas combined with replacement

586 and upgrade of equipment would address the primary sources of Romanian O&G
587 emissions. Further reductions can be achieved by identifying and repairing equipment
588 leaks through frequent monitoring of methane emissions and implementation of leak
589 detection and repair programs. Focusing on these mitigation actions would be an
590 effective and efficient strategy to achieve substantial methane reductions.

591

592 **Data availability**

593 The emission rates dataset used in this study is presented in Table S16 in the Supplementary
594 Material.

595

596 **Author contributions**

597 Study design: TR, HC, MS, JMN, AnC

598

599 Execution and planning of ground and drone based measurements: KV, BK, MdV, SvH, PK, MS,
600 JW, PJ, JMN, JB, HM, MM, CvdV, BT, JR, RPM, LE, DB, MS, AH, IV, PvdB, HDvdG, AD, MEE, CS,
601 MC, SI, DM, AS, AT, IV, AnC, MA, SG, AP, AuC, LC, AN, CB, CP, AR, AM, HS, AD, BH, SS, DZA, HC,
602 TR

603

604 Data evaluation: FS, KV, PK, MS, PJ, JMN, JB, HM, BT, JR, RPM, LE, AH, IV, HDvdG, AD, CS, AnC,
605 SS, DZA, HC, TR

606

607 Preparation of manuscript: FS, DZA, KV, HC, TR with input from PK, MS, PJ, JMN, JB, HM, BT,
608 LE, AH, IV, HDvdG, AD, CS, AnC, SS

609

610 **Acknowledgements**

611 Our collected data, funded by UNEP's International Methane Emissions Observatory (IMEO) is
612 part of a science studies programme that aims to support methane emission mitigation
613 strategies, actions and policies.

614

615 **Funding**

616 The Romanian Methane Emission from Oil & Gas (ROME0) campaign was initiated and largely
617 carried out by participants of the European H2020 project MEMO² (MEthane goes MOBILE -
618 MEasurements and Modelling), which was funded by the European Union's Horizon 2020
619 research and innovation programme under the Marie Skłodowska-Curie grant agreement No.
620 722479. Additional funding was provided by the Climate and Clean Air Coalition (CCAC) Oil &
621 Gas Methane Science Studies (MSS), administered through United Nations Environment
622 Programme (UNEP) under grant number PCA/ CCAC/UU/DTIE19-EN652.

623

624 **Competing interests**

625 The authors declare that they have no conflict of interest.

626

627 **References**

628 Allen, D. T., Torres, V. M., Thomas, J., Sullivan, D. W., Harrison, M., Hendler, A., Herndon, S. C., Kolb, C. E., Fraser,
629 M. P., Hill, A. D., Lamb, B. K., Miskimins, J., Sawyer, R. F., and Seinfeld, J. H.: Measurements of methane emissions
630 at natural gas production sites in the United States, *Proc. Natl. Acad. Sci.*, 110, 17768–17773,
631 <https://doi.org/10.1073/pnas.1304880110>, 2013.

632 Allen, G., Hollingsworth, P., Kabbabe, K., Pitt, J. R., Mead, M. I., Illingworth, S., Roberts, G., Bourn, M., Shallcross,
633 D. E., and Percival, C. J.: The development and trial of an unmanned aerial system for the measurement of
634 methane flux from landfill and greenhouse gas emission hotspots, *Waste Manag.*, 87, 883–892,
635 <https://doi.org/10.1016/j.wasman.2017.12.024>, 2019.

636 Alvarez, R. A., Zavala-Araiza, D., Lyon, D. R., Allen, D. T., Barkley, Z. R., Brandt, A. R., Davis, K. J., Herndon, S. C.,
637 Jacob, D. J., Karion, A., Kort, E. A., Lamb, B. K., Lauvaux, T., Maasakkers, J. D., Marchese, A. J., Omara, M., Pacala,
638 S. W., Peischl, J., Robinson, A. L., Shepson, P. B., Sweeney, C., Townsend-Small, A., Wofsy, S. C., and Hamburg, S.
639 P.: Assessment of methane emissions from the U.S. oil and gas supply chain, *Science*, 361, 186–188,
640 <https://doi.org/10.1126/science.aar7204>, 2018.

641 Andersen, T., Scheeren, B., Peters, W., and Chen, H.: A UAV-based active AirCore system for measurements of
642 greenhouse gases, *Atmospheric Meas. Tech.*, 11, 2683–2699, <https://doi.org/10.5194/amt-11-2683-2018>, 2018.

643 Baray, S., Darlington, A., Gordon, M., Hayden, K. L., Leithead, A., Li, S.-M., Liu, P. S. K., Mittermeier, R. L., Moussa,
644 S. G., O'Brien, J., Staebler, R., Wolde, M., Worthy, D., and McLaren, R.: Quantification of methane sources in the
645 Athabasca Oil Sands Region of Alberta by aircraft mass balance, *Atmospheric Chem. Phys.*, 18, 7361–7378,
646 <https://doi.org/10.5194/acp-18-7361-2018>, 2018.

647 BP: Statistical Review of World Energy 2022 (71st edition), BP, 2022.

648 Brandt, A. R., Heath, G. A., and Cooley, D.: Methane Leaks from Natural Gas Systems Follow Extreme
649 Distributions, *Environ. Sci. Technol.*, 50, 12512–12520, <https://doi.org/10.1021/acs.est.6b04303>, 2016.

650 Brantley, H. L., Thoma, E. D., Squier, W. C., Guven, B. B., and Lyon, D.: Assessment of Methane Emissions from
651 Oil and Gas Production Pads using Mobile Measurements, *Environ. Sci. Technol.*, 48, 14508–14515,
652 <https://doi.org/10.1021/es503070q>, 2014.

653 Delre, A., Mønster, J., and Scheutz, C.: Greenhouse gas emission quantification from wastewater treatment
654 plants, using a tracer gas dispersion method, *Sci. Total Environ.*, 605–606, 258–268,
655 <https://doi.org/10.1016/j.scitotenv.2017.06.177>, 2017.

656 Delre, A., Hensen, A., Velzeboer, I., van den Bulk, P., Edjabou, M. E., and Scheutz, C.: Methane and ethane
657 emission quantifications from onshore oil and gas sites in Romania, using a tracer gas dispersion method, *Elem.*
658 *Sci. Anthr.*, 10, 000111, <https://doi.org/10.1525/elementa.2021.000111>, 2022.

659 Doujaiji, B. and Al, -Tawfiq Jaffar A.: Hydrogen sulfide exposure in an adult male, *Ann. Saudi Med.*, 30, 76–80,
660 <https://doi.org/10.4103/0256-4947.59379>, 2010.

661 Eggleston, H. S., Buendia, L., Miwa, K., Ngara, T., and Tanabe, K.: 2006 IPCC Guidelines for National Greenhouse
662 Gas Inventories, 2006.

663 European Commission: COMMUNICATION FROM THE COMMISSION TO THE EUROPEAN PARLIAMENT, THE
664 COUNCIL, THE EUROPEAN ECONOMIC AND SOCIAL COMMITTEE AND THE COMMITTEE OF THE REGIONS on an
665 EU strategy to reduce methane emissions, 2020.

666 European Commission: Proposal for a REGULATION OF THE EUROPEAN PARLIAMENT AND OF THE COUNCIL on
667 methane emissions reduction in the energy sector and amending Regulation (EU) 2019/942, 2021.

668 Foulds, A., Allen, G., Shaw, J. T., Bateson, P., Barker, P. A., Huang, L., Pitt, J. R., Lee, J. D., Wilde, S. E., Dominutti,
669 P., Purvis, R. M., Lowry, D., France, J. L., Fisher, R. E., Fiehn, A., Pühl, M., Bauguitte, S. J. B., Conley, S. A., Smith,
670 M. L., Lachlan-Cope, T., Pisso, I., and Schwietzke, S.: Quantification and assessment of methane emissions from
671 offshore oil and gas facilities on the Norwegian Continental Shelf, *Atmospheric Chem. Phys.*,
672 <https://doi.org/10.5194/acp-2021-872>, 2022.

673 Gorchov Negron, A. M., Kort, E. A., Conley, S. A., and Smith, M. L.: Airborne Assessment of Methane Emissions
674 from Offshore Platforms in the U.S. Gulf of Mexico, *Environ. Sci. Technol.*, 54, 5112–5120,
675 <https://doi.org/10.1021/acs.est.0c00179>, 2020.

676 Hanna, S. R., Briggs, G. A., and Hosker, J.: Handbook on atmospheric diffusion, National Oceanic and Atmospheric
677 Administration, Oak Ridge, TN (USA). Atmospheric Turbulence and Diffusion Lab.,
678 <https://doi.org/10.2172/5591108>, 1982.

679 IEA: <https://www.iea.org/reports/global-methane-tracker-2022>, last access: 2 November 2022.

680 Methane Tracker Data Explorer: <https://www.iea.org/data-and-statistics/data-tools/methane-tracker-data-explorer>, last access: 2 November 2022.

682 Karion, A., Sweeney, C., Pétron, G., Frost, G., Michael Hardesty, R., Kofler, J., Miller, B. R., Newberger, T., Wolter,
683 S., Banta, R., Brewer, A., Dlugokencky, E., Lang, P., Montzka, S. A., Schnell, R., Tans, P., Trainer, M., Zamora, R.,
684 and Conley, S.: Methane emissions estimate from airborne measurements over a western United States natural
685 gas field, *Geophys. Res. Lett.*, 40, 4393–4397, <https://doi.org/10.1002/grl.50811>, 2013.

686 Korbeń, P., Jagoda, P., Maazallahi, H., Kammerer, J., Nećki, J. M., Wietzel, J. B., Bartyzel, J., Radovici, A., Zavala-
687 Araiza, D., Röckmann, T., and Schmidt, M.: Quantification of methane emission rate from oil and gas wells in
688 Romania using ground-based measurement techniques, *Elem. Sci. Anthr.*, 10, 00070,
689 <https://doi.org/10.1525/elementa.2022.00070>, 2022.

690 Lamb, B. K., McManus, J. B., Shorter, J. H., Kolb, C. E., Mosher, Byard., Harriss, R. C., Allwine, Eugene., Blaha,
691 Denise., Howard, Touche., Guenther, Alex., Lott, R. A., Siverson, Robert., Westburg, Hal., and Zimmerman, Pat.:
692 Development of Atmospheric Tracer Methods To Measure Methane Emissions from Natural Gas Facilities and
693 Urban Areas, *Environ. Sci. Technol.*, 29, 1468–1479, <https://doi.org/10.1021/es00006a007>, 1995.

694 Lavoie, M., Baillie, J., Bourlon, E., O’Connell, E., MacKay, K., Boelens, I., and Risk, D.: Sweet and sour: A
695 quantitative analysis of methane emissions in contrasting Alberta, Canada, heavy oil developments, *Sci. Total
696 Environ.*, 807, 150836, <https://doi.org/10.1016/j.scitotenv.2021.150836>, 2022.

697 MacKay, K., Lavoie, M., Bourlon, E., Atherton, E., O’Connell, E., Baillie, J., Fougère, C., and Risk, D.: Methane
698 emissions from upstream oil and gas production in Canada are underestimated, *Sci. Rep.*, 11, 8041,
699 <https://doi.org/10.1038/s41598-021-87610-3>, 2021.

700 Marriott, R. A., Pirzadeh, P., Marrugo-Hernandez, J. J., and Raval, S.: Hydrogen sulfide formation in oil and gas,
701 *Can. J. Chem.*, 94, 406–413, <https://doi.org/10.1139/cjc-2015-0425>, 2016.

702 Morales, R., Ravelid, J., Vinkovic, K., Korbeń, P., Tuzson, B., Emmenegger, L., Chen, H., Schmidt, M., Humbel, S.,
703 and Brunner, D.: Controlled-release experiment to investigate uncertainties in UAV-based emission
704 quantification for methane point sources, *Atmospheric Meas. Tech.*, 15, 2177–2198,
705 <https://doi.org/10.5194/amt-15-2177-2022>, 2022.

706 Nathan, B. J., Golston, L. M., O’Brien, A. S., Ross, K., Harrison, W. A., Tao, L., Lary, D. J., Johnson, D. R., Covington,
707 A. N., Clark, N. N., and Zondlo, M. A.: Near-Field Characterization of Methane Emission Variability from a
708 Compressor Station Using a Model Aircraft, *Environ. Sci. Technol.*, 49, 7896–7903,
709 <https://doi.org/10.1021/acs.est.5b00705>, 2015.

710 Ocko, I. B., Sun, T., Shindell, D., Oppenheimer, M., Hristov, A. N., Pacala, S. W., Mauzerall, D. L., Xu, Y., and
711 Hamburg, S. P.: Acting rapidly to deploy readily available methane mitigation measures by sector can
712 immediately slow global warming, *Environ. Res. Lett.*, 16, 054042, <https://doi.org/10.1088/1748-9326/abf9c8>,
713 2021.

714 Omara, M., Sullivan, M. R., Li, X., Subramanian, R., Robinson, A. L., and Presto, A. A.: Methane Emissions from
715 Conventional and Unconventional Natural Gas Production Sites in the Marcellus Shale Basin, *Environ. Sci.
716 Technol.*, 50, 2099–2107, <https://doi.org/10.1021/acs.est.5b05503>, 2016.

717 O’Shea, S. J., Allen, G., Gallagher, M. W., Bower, K., Illingworth, S. M., Muller, J. B. A., Jones, B. T., Percival, C. J.,
718 Bauguitte, S. J.-B., Cain, M., Warwick, N., Quiquet, A., Skiba, U., Drewer, J., Dinsmore, K., Nisbet, E. G., Lowry, D.,
719 Fisher, R. E., France, J. L., Aurela, M., Lohila, A., Hayman, G., George, C., Clark, D. B., Manning, A. J., Friend, A. D.,
720 and Pyle, J.: Methane and carbon dioxide fluxes and their regional scalability for the European Arctic wetlands

721 during the MAMM project in summer 2012, *Atmospheric Chem. Phys.*, 14, 13159–13174,
722 <https://doi.org/10.5194/acp-14-13159-2014>, 2014.

723 Pitt, J. R., Allen, G., Bauguitte, S. J.-B., Gallagher, M. W., Lee, J. D., Drysdale, W., Nelson, B., Manning, A. J., and
724 Palmer, P. I.: Assessing London CO₂, CH₄ and CO emissions using aircraft measurements and dispersion modelling,
725 *Atmospheric Chem. Phys.*, 19, 8931–8945, <https://doi.org/10.5194/acp-19-8931-2019>, 2019.

726 Rella, C. W., Tsai, T. R., Botkin, C. G., Crosson, E. R., and Steele, D.: Measuring Emissions from Oil and Natural Gas
727 Well Pads Using the Mobile Flux Plane Technique, *Environ. Sci. Technol.*, 49, 4742–4748,
728 <https://doi.org/10.1021/acs.est.5b00099>, 2015.

729 Riddick, S. N., Connors, S., Robinson, A. D., Manning, A. J., Jones, P. S. D., Lowry, D., Nisbet, E., Skelton, R. L., Allen,
730 G., Pitt, J., and Harris, N. R. P.: Estimating the size of a methane emission point source at different scales: from
731 local to landscape, *Atmospheric Chem. Phys.*, 17, 7839–7851, <https://doi.org/10.5194/acp-17-7839-2017>, 2017.

732 Riddick, S. N., Mauzerall, D. L., Celia, M. A., Kang, M., Bressler, K., Chu, C., and Gum, C. D.: Measuring methane
733 emissions from abandoned and active oil and gas wells in West Virginia, *Sci. Total Environ.*, 651, 1849–1856,
734 <https://doi.org/10.1016/j.scitotenv.2018.10.082>, 2019.

735 Robertson, A. M., Edie, R., Snare, D., Soltis, J., Field, R. A., Burkhart, M. D., Bell, C. S., Zimmerle, D., and Murphy,
736 S. M.: Variation in Methane Emission Rates from Well Pads in Four Oil and Gas Basins with Contrasting Production
737 Volumes and Compositions, *Environ. Sci. Technol.*, 51, 8832–8840, <https://doi.org/10.1021/acs.est.7b00571>,
738 2017.

739 Robertson, A. M., Edie, R., Field, R. A., Lyon, D., McVay, R., Omara, M., Zavala-Araiza, D., and Murphy, S. M.: New
740 Mexico Permian Basin Measured Well Pad Methane Emissions Are a Factor of 5–9 Times Higher Than U.S. EPA
741 Estimates, *Environ. Sci. Technol.*, 54, 13926–13934, <https://doi.org/10.1021/acs.est.0c02927>, 2020.

742 Röckmann, T.: ROMEO-ROmanian Methane Emissions from Oil and Gas, in: EGU General Assembly Conference
743 Abstracts, 18801, 2020.

744 Roscioli, J. R., Yacovitch, T. I., Floerchinger, C., Mitchell, A. L., Tkacik, D. S., Subramanian, R., Martinez, D. M.,
745 Vaughn, T. L., Williams, L., Zimmerle, D., Robinson, A. L., Herndon, S. C., and Marchese, A. J.: Measurements of
746 methane emissions from natural gas gathering facilities and processing plants: measurement methods,
747 *Atmospheric Meas. Tech.*, 8, 2017–2035, <https://doi.org/10.5194/amt-8-2017-2015>, 2015.

748 Rutherford, J. S., Sherwin, E. D., Ravikumar, A. P., Heath, G. A., Englander, J., Cooley, D., Lyon, D., Omara, M.,
749 Langfitt, Q., and Brandt, A. R.: Closing the methane gap in US oil and natural gas production emissions inventories,
750 *Nat. Commun.*, 12, 4715, <https://doi.org/10.1038/s41467-021-25017-4>, 2021.

751 Saunio, M., Stavert, A. R., Poulter, B., Bousquet, P., Canadell, J. G., Jackson, R. B., Raymond, P. A., Dlugokencky,
752 E. J., Houweling, S., Patra, P. K., Ciais, P., Arora, V. K., Bastviken, D., Bergamaschi, P., Blake, D. R., Brailsford, G.,
753 Bruhwiler, L., Carlson, K. M., Carrol, M., Castaldi, S., Chandra, N., Crevoisier, C., Crill, P. M., Covey, K., Curry, C. L.,
754 Etioppe, G., Frankenberg, C., Gedney, N., Hegglin, M. I., Höglund-Isaksson, L., Hugelius, G., Ishizawa, M., Ito, A.,
755 Janssens-Maenhout, G., Jensen, K. M., Joos, F., Kleinen, T., Krummel, P. B., Langenfelds, R. L., Laruelle, G. G., Liu,
756 L., Machida, T., Maksyutov, S., McDonald, K. C., McNorton, J., Miller, P. A., Melton, J. R., Morino, I., Müller, J.,
757 Murguía-Flores, F., Naik, V., Niwa, Y., Noce, S., O’Doherty, S., Parker, R. J., Peng, C., Peng, S., Peters, G. P., Prigent,
758 C., Prinn, R., Ramonet, M., Regnier, P., Riley, W. J., Rosentreter, J. A., Segers, A., Simpson, I. J., Shi, H., Smith, S.
759 J., Steele, L. P., Thornton, B. F., Tian, H., Tohjima, Y., Tubiello, F. N., Tsuruta, A., Viovy, N., Voulgarakis, A., Weber,
760 T. S., van Weele, M., van der Werf, G. R., Weiss, R. F., Worthy, D., Wunch, D., Yin, Y., Yoshida, Y., Zhang, W.,
761 Zhang, Z., Zhao, Y., Zheng, B., Zhu, Q., Zhu, Q., and Zhuang, Q.: The Global Methane Budget 2000–2017, *Earth
762 Syst. Sci. Data*, 12, 1561–1623, <https://doi.org/10.5194/essd-12-1561-2020>, 2020.

763 Shah, A., Ricketts, H., Pitt, J. R., Shaw, J. T., Kabbabe, K., Leen, J. B., and Allen, G.: Unmanned aerial vehicle
764 observations of cold venting from exploratory hydraulic fracturing in the United Kingdom, *Environ. Res.
765 Commun.*, 2, 021003, <https://doi.org/10.1088/2515-7620/ab716d>, 2020.

766 Shen, L., Zavala-Araiza, D., Gautam, R., Omara, M., Scarpelli, T., Sheng, J., Sulprizio, M. P., Zhuang, J., Zhang, Y.,
767 Qu, Z., Lu, X., Hamburg, S. P., and Jacob, D. J.: Unravelling a large methane emission discrepancy in Mexico using
768 satellite observations, *Remote Sens. Environ.*, 260, 112461, <https://doi.org/10.1016/j.rse.2021.112461>, 2021.

769 Shi, T., Han, Z., Han, G., Ma, X., Chen, H., Andersen, T., Mao, H., Chen, C., Zhang, H., and Gong, W.: Retrieving
770 CH₄-emission rates from coal mine ventilation shafts using UAV-based AirCore observations and the genetic
771 algorithm–interior point penalty function (GA-IPPF) model, *Atmospheric Chem. Phys.*, 22, 13881–13896,
772 <https://doi.org/10.5194/acp-22-13881-2022>, 2022.

773 Szopa, S., Naik, V., Adhikary, B., Artaxo, P., Berntsen, T., Collins, W. D., Fuzzi, S., Gallardo, L., Kiendler-Scharr, A.,
774 Klimont, Z., Liao, H., Unger, N., and Zanis, P.: Short-Lived Climate Forcers, *Clim. Change 2021 Phys. Sci. Basis*
775 *Contrib. Work. Group Sixth Assess. Rep. Intergov. Panel Clim. Change Camb. Univ. Press Camb. U. K. N. Y. NY USA*,
776 817–922, 2021.

777 Thoma, E. and Squier, B.: OTM 33 geospatial measurement of air pollution, remote emissions quantification
778 (gmap-req) and OTM33A geospatial measurement of air pollution-remote emissions quantification-direct
779 assessment (GMAP-REQ-DA), US Environ. Prot. Agency Cincinnati OH, 2014.

780 Tuzson, B., Graf, M., Ravelid, J., Scheidegger, P., Kupferschmid, A., Looser, H., Morales, R. P., and Emmenegger,
781 L.: A compact QCL spectrometer for mobile, high-precision methane sensing aboard drones, *Atmospheric Meas.*
782 *Tech.*, 13, 4715–4726, <https://doi.org/10.5194/amt-13-4715-2020>, 2020.

783 Tyner, D. R. and Johnson, M. R.: Where the Methane Is—Insights from Novel Airborne LiDAR Measurements
784 Combined with Ground Survey Data, *Environ. Sci. Technol.*, 55, 9773–9783,
785 <https://doi.org/10.1021/acs.est.1c01572>, 2021.

786 Greenhouse Gas Inventory Data - Comparison by Category: https://di.unfccc.int/comparison_by_category, last
787 access: 2 November 2022.

788 Vinković, K., Andersen, T., de Vries, M., Kers, B., van Heuven, S., Peters, W., Hensen, A., van den Bulk, P., and
789 Chen, H.: Evaluating the use of an Unmanned Aerial Vehicle (UAV)-based active AirCore system to quantify
790 methane emissions from dairy cows, *Sci. Total Environ.*, 831, 154898,
791 <https://doi.org/10.1016/j.scitotenv.2022.154898>, 2022.

792 Yacovitch, T. I., Daube, C., Vaughn, T. L., Bell, C. S., Roscioli, J. R., Knighton, W. B., Nelson, D. D., Zimmerle, D.,
793 Pétron, G., and Herndon, S. C.: Natural gas facility methane emissions: measurements by tracer flux ratio in two
794 US natural gas producing basins, *Elem. Sci. Anthr.*, 5, 69, <https://doi.org/10.1525/elementa.251>, 2017.

795 Yacovitch, T. I., Neining, B., Herndon, S. C., van der Gon, H. D., Jonkers, S., Hulskotte, J., Roscioli, J. R., and
796 Zavala-Araiza, D.: Methane emissions in the Netherlands: The Groningen field, *Elem. Sci. Anthr.*, 6, 57,
797 <https://doi.org/10.1525/elementa.308>, 2018.

798 Zavala-Araiza, D., Lyon, D. R., Alvarez, R. A., Davis, K. J., Harriss, R., Herndon, S. C., Karion, A., Kort, E. A., Lamb, B.,
799 K., Lan, X., Marchese, A. J., Pacala, S. W., Robinson, A. L., Shepson, P. B., Sweeney, C., Talbot, R., Townsend-Small,
800 A., Yacovitch, T. I., Zimmerle, D. J., and Hamburg, S. P.: Reconciling divergent estimates of oil and gas methane
801 emissions, *Proc. Natl. Acad. Sci.*, 112, 15597–15602, <https://doi.org/10.1073/pnas.1522126112>, 2015.

802 Zavala-Araiza, D., Alvarez, R. A., Lyon, D. R., Allen, D. T., Marchese, A. J., Zimmerle, D. J., and Hamburg, S. P.:
803 Super-emitters in natural gas infrastructure are caused by abnormal process conditions, *Nat. Commun.*, 8, 14012,
804 <https://doi.org/10.1038/ncomms14012>, 2017.

805 Zavala-Araiza, D., Herndon, S. C., Roscioli, J. R., Yacovitch, T. I., Johnson, M. R., Tyner, D. R., Omara, M., and
806 Knighton, B.: Methane emissions from oil and gas production sites in Alberta, Canada, *Elem. Sci. Anthr.*, 6, 27,
807 <https://doi.org/10.1525/elementa.284>, 2018.

808 Zavala-Araiza, D., Omara, M., Gautam, R., Smith, M. L., Pandey, S., Aben, I., Almanza-Veloz, V., Conley, S.,
809 Houweling, S., Kort, E. A., Maasakkers, J. D., Molina, L. T., Pusuluri, A., Scarpelli, T., Schwietzke, S., Shen, L., Zavala,

810 M., and Hamburg, S. P.: A tale of two regions: methane emissions from oil and gas production in
811 offshore/onshore Mexico, *Environ. Res. Lett.*, 16, 024019, <https://doi.org/10.1088/1748-9326/abceeb>, 2021.